HiSST: 4th International Conference on High-Speed Vehicle Science & Technology
22–26 September 2025, Tours, France

Low-cost supersonic combustion modeling for hydrogen transverse injection

Pedro P. B. Araújo[1], *Yan S. Pedroni*[2], *Amanda C. Romano*[3],
João V. M. B. Siqueira[4], *Leda M. Vialta*[5], *Fábio H. E. Ribeiro*[6], *Angelo Passaro*[7]

Abstract

This study presents a comparison between a low-cost supersonic combustion modeling approach and CFD simulations validated against experimental data obtained from shock tunnel testing. The CFD analysis employs a finite-rate chemistry model without turbulence-chemistry interaction (no TCI), using the SST k–ω turbulence model in a Reynolds-Averaged Navier-Stokes equation (RANS) approach. Three combustor geometries, with and without flame holder, were evaluated. Parameters of combustion efficiency were derived from CFD simulations. Pressure, temperature, and Mach number were compared to assess the accuracy of the proposed low-cost methodology.

Keywords: *Supersonic combustion, low-cost tool, combustion efficiency, cavity*

1. Introduction

Scramjet engines are promising hypersonic airbreathing propulsion systems for space access, allowing supersonic combustion with atmospheric air in the combustion chamber. Due to its importance for military and civilian applications, it has received significant attention over the past decades. Computational fluid dynamics (CFD) simulations and shock tunnel experiments have been widely used for supersonic combustion analyses.

Using computational fluid dynamics (CFD) simulation tools offers enhanced flexibility for studying parameter variations. CFD allows easier test conditions and geometrical modifications than shock tunnel experiments. An additional advantage of CFD is the possibility of evaluating a range of parameters, such as combustion and mixing efficiencies, and thrust gain, without relying on physical apparatus that might affect the flow or be unavailable. However, numerically solving the governing equations alone does not guarantee that the physics is accurately captured, making validation with experimental data essential.

Although CFD has been widely used to study supersonic combustion, the computational cost is a limitation for evaluating thousands of configurations in an optimization process. For a preliminary de-

[1] *Institute for Advanced Studies, Trevo Coronel Aviador José Alberto Albano do Amarante, 1 – São José dos Campos/SP – Brazil, araujo.projects@gmail.com*
[2] *Institute for Advanced Studies, Trevo Coronel Aviador José Alberto Albano do Amarante, 1 – São José dos Campos/SP – Brazil, bolsa30.ieav@fab.mil.br*
[3] *Institute for Advanced Studies, Trevo Coronel Aviador José Alberto Albano do Amarante, 1 – São José dos Campos/SP – Brazil, bolsa12.ieav@fab.mil.br*
[4] *Institute for Advanced Studies, Trevo Coronel Aviador José Alberto Albano do Amarante, 1 – São José dos Campos/SP – Brazil, bolsa24.ieav@fab.mil.br*
[5] *Institute for Advanced Studies, Trevo Coronel Aviador José Alberto Albano do Amarante, 1 – São José dos Campos/SP – Brazil, bolsa20.ieav@fab.mil.br*
[6] *Institute for Advanced Studies, Trevo Coronel Aviador José Alberto Albano do Amarante, 1 – São José dos Campos/SP – Brazil, henriquefher@fab.mil.br*
[7] *Institute for Advanced Studies, Trevo Coronel Aviador José Alberto Albano do Amarante, 1 – São José dos Campos/SP – Brazil, angelopassaro@gmail.com*

Copyright © 2025 by the author(s)

sign analysis, we are looking for low-cost tools to perform optimization and assist in decision-making faster.

The initial design can be accomplished using analytical formulations based on well-established theories, such as oblique shock wave, constant area heat addition, and area ratio [11, 1]. These theories effectively capture the physics of the problem and provide approximate results. Araújo et al. [4, 3] designed a scramjet engine through an optimization approach employing low-cost methods, achieving good agreement with CFD results. Carneiro, Passaro, and Toro [7] presented a methodology for estimating flow properties in a variable-area combustor by coupling Rayleigh flow theory with geometric area variation.

Birzer and Doolan [6] presented a strut-based model for supersonic combustion efficiency with calibrated parameters derived from the results of the CFD simulation in Gerlinger and Bruggemann [10]. Bezerra et al. [5] conducted a numerical investigation of hydrogen transverse injection into supersonic airflow within a combustion chamber featuring a variable cross-sectional area. The study employed compressible 2D RANS simulations coupled with simplified chemical kinetics to assess various injection configurations. Inlet flow properties were assumed constant at the combustor entrance, with air modeled as a calorically perfect gas. Hydrogen was injected at sonic velocity, maintaining the same mass flow rate for both single and double injection cases. Ogawa and Boyce [14] performed a multiobjective design optimization of an axisymmetric scramjet inlet based on evolutionary algorithms with respect to four main inlet design criteria: compression efficiency, drag, adverse pressure gradient, and exit temperature. The first three criteria are used as the objective functions, and the last is a constraint function. Multi-objective optimization is performed using CFD for aerodynamic evaluation, which has a significant computational cost.

This study aims to validate the CFD simulations against experimental data from the shock tunnel in Brazil [17, 18] (Table 1) and to compare the data with a novel low-cost combustion modeling approach that considers pressure loss due to viscous effects, comparing different friction coefficients. The combustion efficiency obtained from the CFD results is employed to calibrate the parameters of the η_c model. The accuracy of the proposed low-cost methodology is evaluated by comparing the mass-weighted averages of pressure, temperature, and Mach number from CFD data against the low-cost tool's estimation.

Table 1. Air inlet and hydrogen injection properties, and the flame holder geometry dimensions for the length and depth ($L \times D$) in millimeters.

Flame holder	**M0**	**M1**	**M5**
L **[mm]** $\times$ D **[mm]**	-	10×5	20×10
Air inlet	**CASE I**	**CASE II**	**CASE III**
Velocity [m/s]	1600	1600	1600
Pressure [Pa]	140000	140000	140000
Temperature [K]	900	900	900
Hydrogen inlet	**CASE I**	**CASE II**	**CASE III**
Velocity [m/s]	1202.18	1202.18	1202.18
Pressure [Pa]	917158.23	917158.23	917158.23
Temperature [K]	248.33	248.33	248.33

2. Methodology

The supersonic combustion is modeled based on the simplified method of Rayleigh's one-dimensional heat addition theory, without fuel addition [11, 1], using the same approach presented in Carneiro, Passaro, and Toro [7] to estimate the flow properties for a variable area combustor without viscous effects.

The conservation equations for mass, momentum, and energy can be applied to one-dimensional

Copyright © 2025 by the author(s)

Rayleigh flow with heat addition, under the assumptions of constant cross-sectional area and no fuel mass addition. This idealization is relevant for modeling supersonic combustion processes within the scramjet combustion chamber (Fig. 1). For a calorically perfect gas, the application of the total temperature definition to the energy equation reveals that heat addition directly affects the total energy of the flow. Consequently, closed-form expressions for the ratios of thermodynamic properties across the flow can be derived by manipulating the governing conservation equations, as follows:

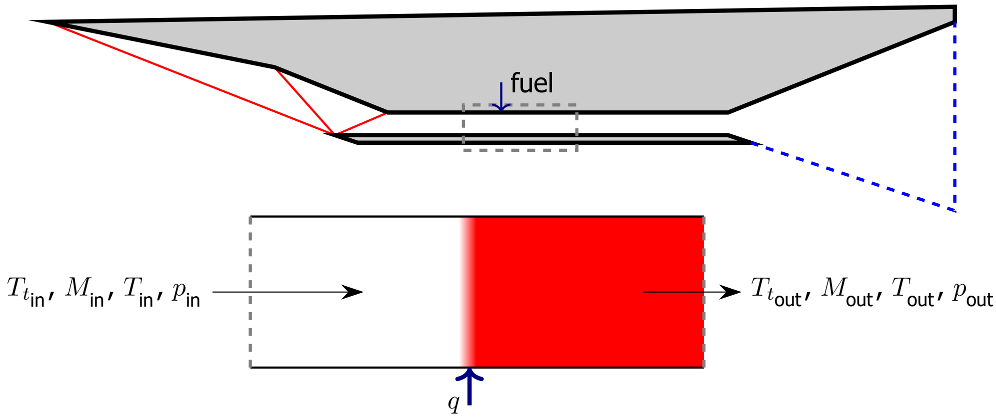

Fig 1. Control volume used in the combustion chamber analyzes where, in a simplified approach, fuel addition is replaced by heat addition.

$$q = c_p \left(T_{t_{\text{out}}} - T_{t_{\text{in}}} \right) \tag{1}$$

$$\frac{T_t}{T} = 1 + \frac{(\gamma - 1)}{2} M^2 \tag{2}$$

$$\frac{p_{\text{out}}}{p_{\text{in}}} = \frac{1 + \gamma M_{\text{in}}^2}{1 + \gamma M_{\text{out}}^2} \tag{3}$$

$$\frac{\rho_{\text{out}}}{\rho_{\text{in}}} = \left(\frac{1 + \gamma M_{\text{out}}^2}{1 + \gamma M_{\text{in}}^2} \right) \left(\frac{M_{\text{in}}}{M_{\text{out}}} \right)^2 \tag{4}$$

$$\frac{T_{\text{out}}}{T_{\text{in}}} = \frac{p_{\text{out}}}{p_{\text{in}}} \frac{\rho_{\text{in}}}{\rho_{\text{out}}} \tag{5}$$

where T_t is the total temperature, c_p is the specific heat at constant pressure, and q is the heat per kilogram added to the flow. The subscripts `in` and `out` refer to the flow properties before and after the heat addition location, respectively (Fig. 1).

The flow from the compression section is deflected to the combustion chamber entrance at supersonic speed, and fuel is injected right after the entrance (Fig. 1) at sonic speed. One-dimensional Rayleigh flow with heat addition may be applied to the combustion process, burning hydrogen (H_2) and oxygen (O_2), increasing the pressure, density, and temperature at the combustion chamber exit, reducing the Mach number, which must remain supersonic to avoid choked flow [1, 11, 4, 8].

Carneiro, Passaro, and Toro [7] segmented the combustion chamber in such a way that each subsection exhibits sufficiently small area variations, thereby justifying the application of the constant-area Rayleigh flow model with heat addition. This approach effectively superimposes the influences of area ratio

Copyright © 2025 by the author(s)

and Rayleigh flow theory, while neglecting total pressure losses due to wall friction. However, their assumption of uniform heat release along the combustor lacks physical fidelity. As shown by Birzer and Doolan [6], modeling heat addition using a combustion efficiency curve yields a more realistic representation of the combustion process in a scramjet combustor. The combustion efficiency is given by:

$$\eta_c = a\left(1 - \exp\left(-(k\,\bar{x})^d\right)\right) \tag{6}$$

$$\bar{x} = \frac{x - x_{\text{inj}}}{L_{\text{mix}}} \tag{7}$$

where $a = 1.06492$, $k = 3.69639$, and $d = 0.80586$ are parameters calibrated for parallel injection in Birzer and Doolan [6]; x_{inj} denotes the streamwise location of the fuel injection point, and L_{mix} represents the corresponding mixing length. For the present work, d and L_{mix} parameters are set for transverse hydrogen injection, derived from CFD.

To incorporate total pressure losses in the duct, the Fanno flow model [1] is integrated with these effects to account for wall friction in the prediction of flow velocity and thermodynamic properties along the combustion chamber.

$$\int_{x_1}^{x_2} \frac{4\,c_f\,dx}{D_h} = \left[-\frac{1}{\gamma M^2} - \frac{\gamma+1}{2\gamma}\ln\left(\frac{M^2}{1+\frac{\gamma-1}{2}M^2}\right)\right]_{M_1}^{M_2} \tag{8}$$

where subscripts 1 and 2 refer to the beginning and end of each subsection into which the combustor is discretized, allowing for the superposition of effects. D_h is the hydraulic diameter, and c_f is the friction coefficient.

Several empirical correlations for the skin friction coefficient can be found in the literature. In the present study, the following models are considered:

- Schlichting and Gersten [16]:

$$c_{f,\text{Gersten}}(Re) = \frac{\lambda}{4}, \quad 1.934\log_{10}(Re\sqrt{\lambda}) - 0.554 - \frac{402}{Re\sqrt{\lambda}} - \frac{1}{\sqrt{\lambda}} = 0 \tag{9}$$

- Prandtl [15]:

$$c_{f,\text{Prandtl}}(Re) = \frac{\lambda}{4}, \quad 2\log_{10}(Re\sqrt{\lambda}) - 0.80 - \frac{1}{\sqrt{\lambda}} = 0 \tag{10}$$

- Meador and Smart [12]:

$$c_{f,\text{Smart}} = \frac{0.02296}{(ReF_{R_x})^{0.139}}\left(\frac{\rho^*}{\rho_e}\right)^{0.861}\left(\frac{\mu^*}{\mu_e}\right)^{0.139} \tag{11}$$

$$T^* = T_e\left(0.5 + 0.032\,M_e^2 + 0.5\frac{T_w}{T_e}\right) \tag{12}$$

- Eckert [9]:

$$c_f = \frac{0.451\,T_e/T^*}{\ln^2\left[0.056\,Re\,(T_e/T^*)^{-0.33}\right]} \tag{13}$$

$$T^* = T_e\left(0.5 + 0.0374\,M_e^2 + 0.5\frac{T_w}{T_e}\right) \tag{14}$$

Copyright © 2025 by the author(s)

In Eq. 11, the reference density ρ^* and dynamic viscosity μ^* are evaluated at the reference temperature T^* (Eq. 12). A modified formulation of the Prandtl friction coefficient, referred to here as *Prandtl modified*, is proposed by replacing the base-10 logarithm in Eq. 10 with the natural logarithm:

$$c_{f,\text{Prandtl mod.}}(Re) = \frac{\lambda}{4}, \quad 2\ln(Re\sqrt{\lambda}) - 0.80 - \frac{1}{\sqrt{\lambda}} = 0 \tag{15}$$

The purpose of this modification is to investigate how the choice of logarithmic formulation affects the friction coefficient predictions and to examine its influence on the evaluation of flow properties in high-speed internal duct flows.

The numerical simulations were carried out by solving the compressible governing equations for mass conservation, species transport, momentum (Navier-Stokes), and energy using the commercial CFD software ANSYS Fluent [2]. Turbulence effects were modeled with the SST $k-\omega$ closure formulation proposed by Menter [13]. The computational domain (Fig. 2) uses a symmetry boundary condition along the midplane of the width. The walls were modeled with a non-slip condition and a fixed temperature of 300 K. At the outlet, static pressure and temperature were prescribed as 0 Pa and 300 K, respectively. Injection and inlet boundary conditions were defined based on the values presented in Table 1. Turbulence parameters at the inlet, injection and outlet were specified using a turbulence intensity of 5% and a turbulent viscosity ratio of 10.

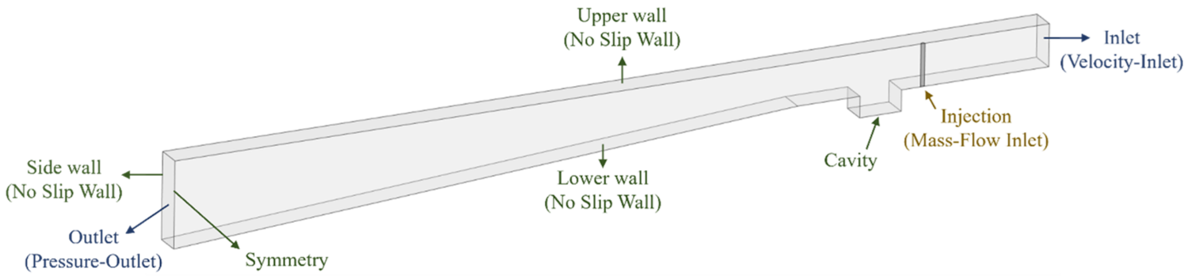

Fig 2. Combustion chamber domain and the boundaries used in the CFD analysis.

The fuel injection is located approximately 14.5% of the total combustor length from the inlet. The cavity begins around 16.8% of the total length, while the divergent section, designed to mitigate back pressure effects, starts at approximately 28.7%.

3. Results

To assess the accuracy of the proposed low-cost methodology for estimating the flow properties along the combustion chamber of a scramjet engine burning hydrogen, it is necessary to compare results with data from experiments in a shock tunnel or from CFD, which is validated with experimental data. Therefore, wall static pressure from computational fluid dynamics simulation were compared with data from a shock tunnel experiment using flame-holders described in Table 1. The parameters L_{mix} and d are derived from CFD simulations for each case and subsequently used to evaluate and compare the pressure, Mach number, and temperature distributions along the combustion chamber against the corresponding CFD results.

3.1. Validation

Comparing the wall static pressure along the combustor central line in the streamwise direction of the CFD simulation against sensor data from the shock tunnel experiment [17, 18] for CASE I, II and III (Table 1 shows good agreement with the pressure behavior in the combustion chamber (Figs. 3-5).

The combustion efficiency increases in the presence of a flame-holder, with the M5 geometry exhibiting the highest efficiency, as shown in Fig.6. This trend is consistent with the findings of Vialta [17], who

Copyright © 2025 by the author(s)

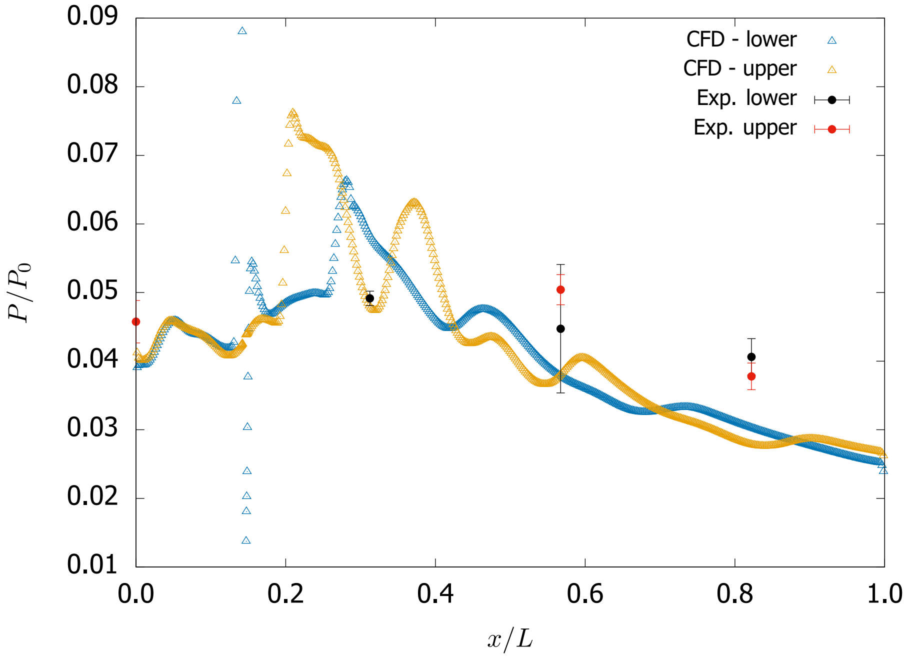

Fig 3. Static pressure comparison between CFD and experiment in shock tunnel for combustor geometry named M0 - CASE I.

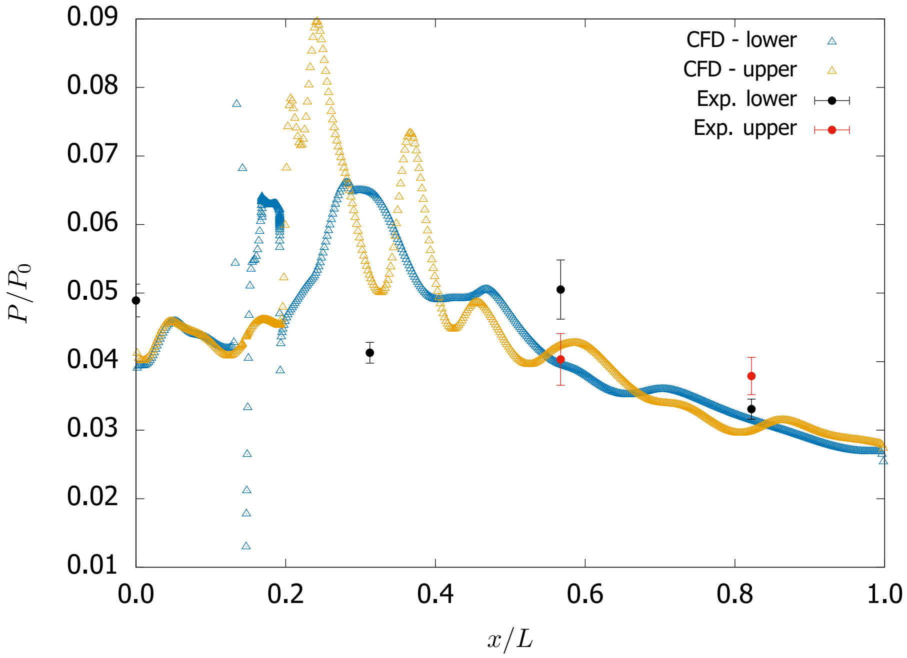

Fig 4. Static pressure comparison between CFD and experiment in shock tunnel for combustor geometry named M1 - CASE II.

Copyright © 2025 by the author(s)

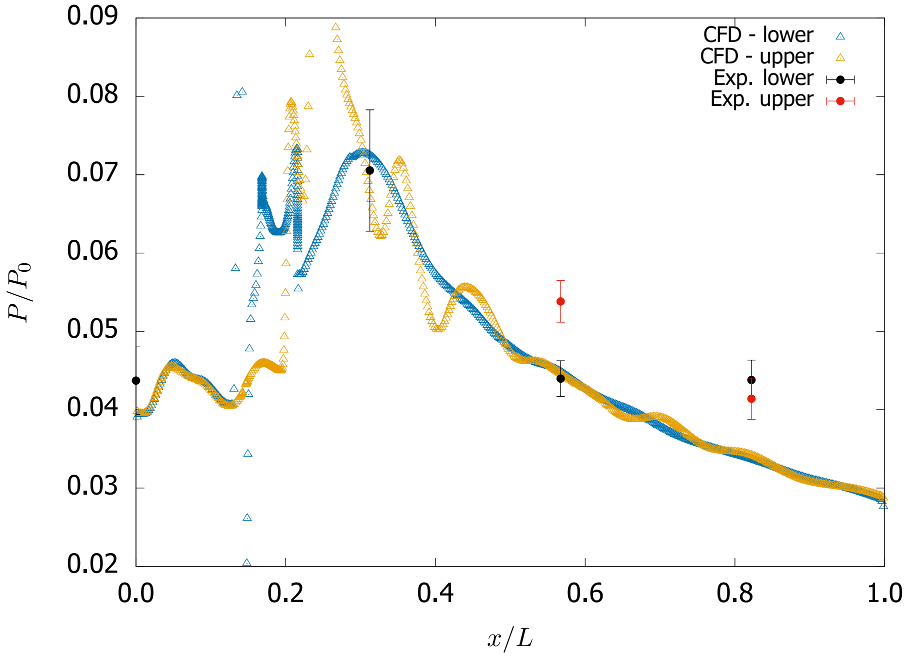

Fig 5. Static pressure comparison between CFD and experiment in shock tunnel for combustor geometry named M5 - CASE III.

reported that OH* emission intensity is enhanced by the use of flame-holders, with the M5 configuration producing the strongest emission. Furthermore, by fitting the L_{mix} and d parameters to the combustion efficiency curves (Fig.6), it is evident that CASE III (M5 geometry) significantly reduces the mixing length, as detailed in Table2.

Table 2. Parameters derived from CFD simulations.

Flame holder	M0	M1	M5
L_{mix} [m]	6.232	4.133	1.546
d	0.505	0.513	0.499

With the adjusted parameters for combustion efficiency in the case of transverse hydrogen injection, the static pressure distribution along the combustion chamber is compared with CFD results to assess the accuracy of the proposed methodology. In the CFD analysis, the static pressure is evaluated using mass-weighted averages along the streamwise direction.

3.2. Low-cost approach

Comparison of the pressure distribution along the combustion chamber with CFD data highlights the critical influence of the selected friction coefficient (Fig. 7–9). All friction models employing base-10 logarithmic formulations tend to overpredict the static pressure relative to the CFD results. Remarkably, the CFD simulations capture a localized pressure rise near the fuel injection point, attributed to the formation of a bow shock induced by the transverse hydrogen injection (Fig. 10), an effect not accounted for in the low-cost methodology. Consequently, an underestimation of pressure is expected in the vicinity of the fuel injection region when using the simplified model. Among the friction models evaluated, only the modified Prandtl formulation, which employs the natural logarithm, demonstrates a pressure distribution that more accurately captures this behavior.

Copyright © 2025 by the author(s)

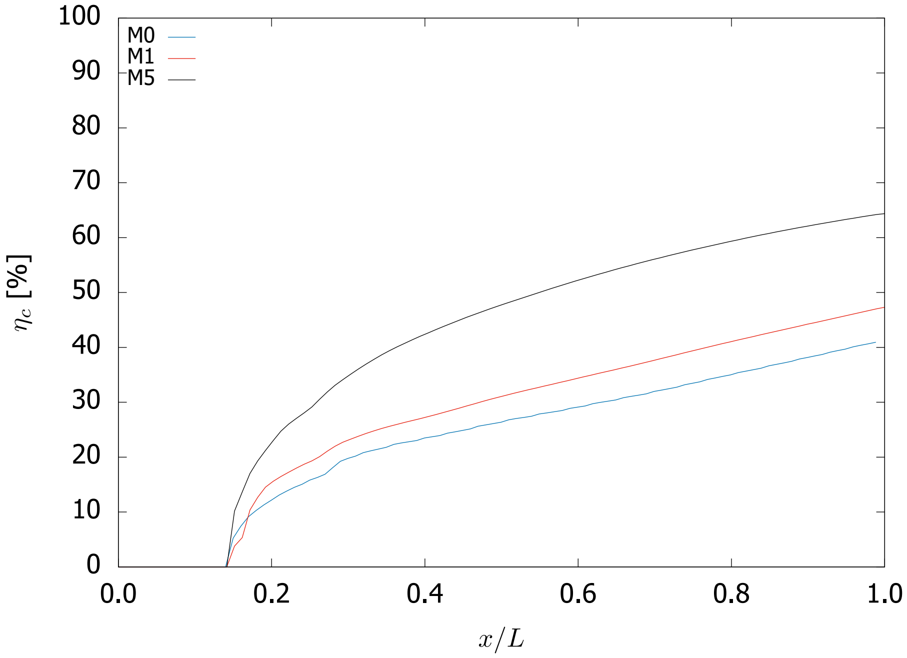

Fig 6. Combustion efficiency for cases analyzed.

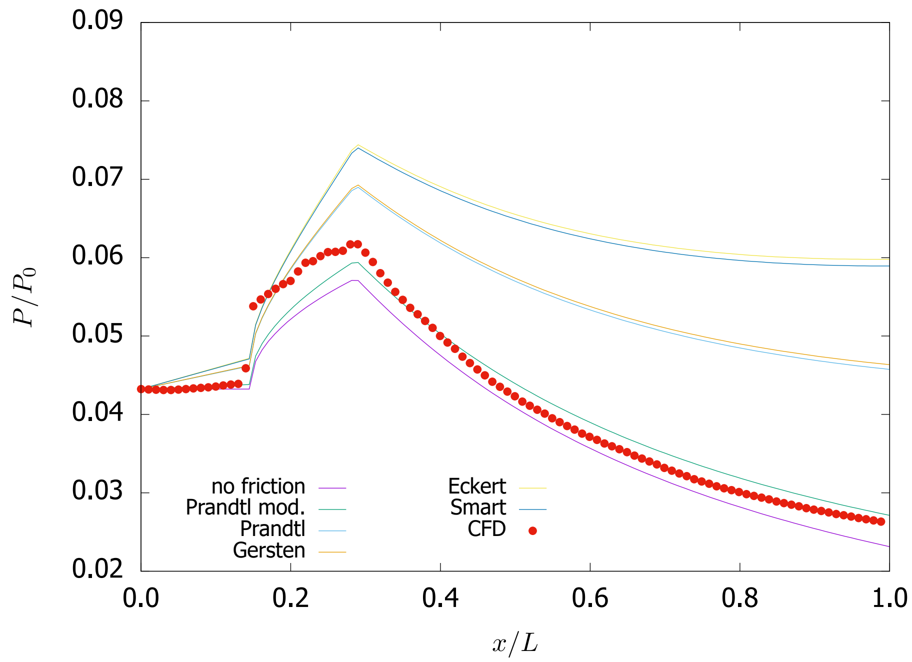

Fig 7. Static pressure comparison between CFD and low-cost combustion model for combustor geometry named M0 - CASE I.

Copyright © 2025 by the author(s)

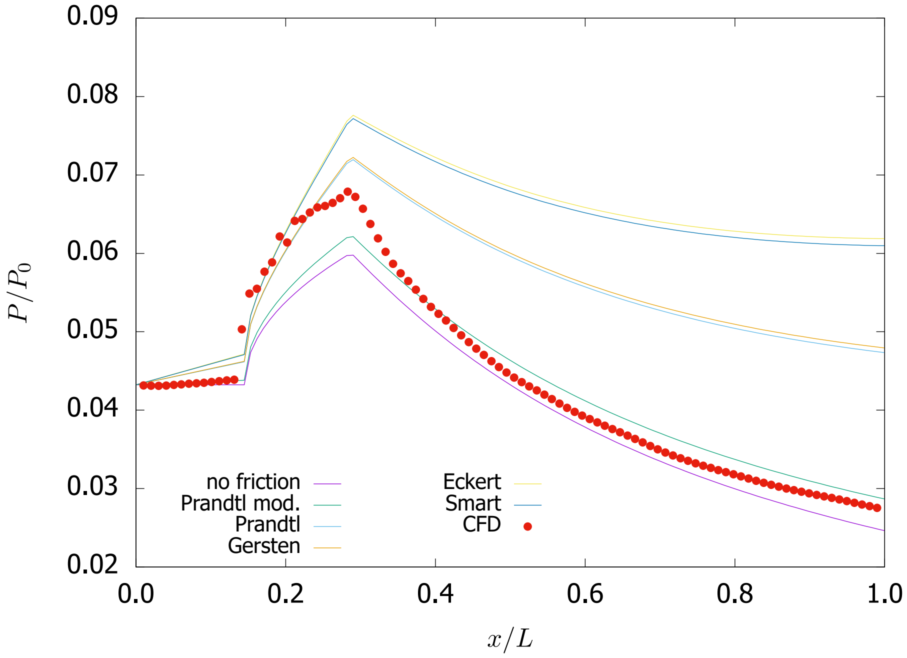

Fig 8. Static pressure comparison between CFD and low-cost combustion model for combustor geometry named M1 - CASE II.

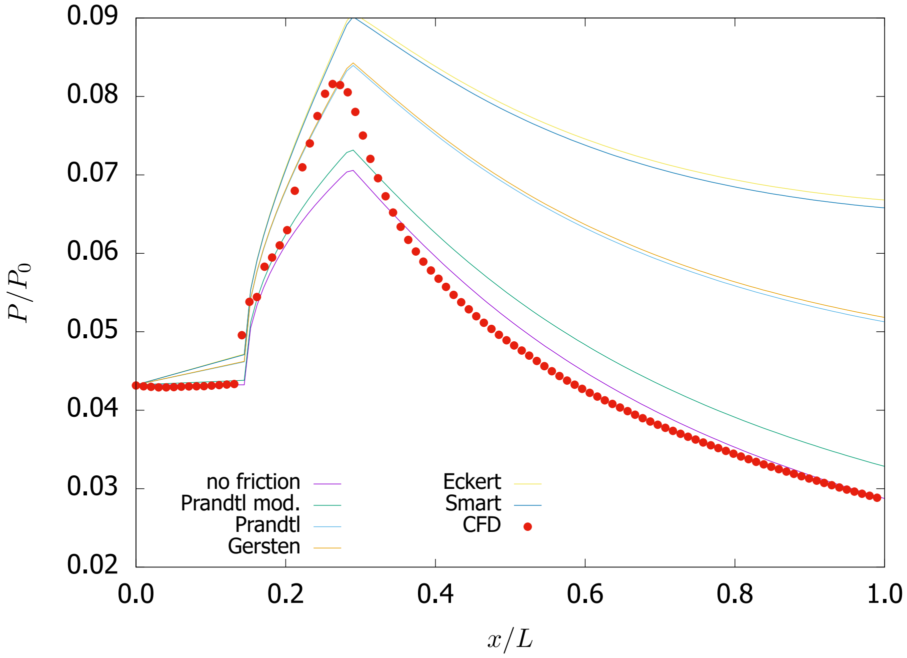

Fig 9. Static pressure comparison between CFD and low-cost combustion model for combustor geometry named M5 - CASE III.

Copyright © 2025 by the author(s)

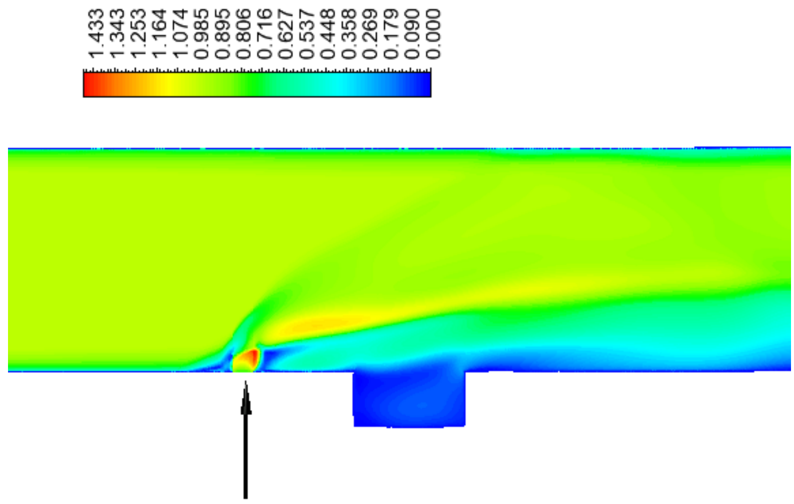

Fig 10. Normalized velocity at the symmetry plane for CASE II - M1 geometry.

For Mach number the behavior is almost the same as the pressure. Comparing the low-cost estimation with the mass-weighted average for Mach number from CFD, the Prandtl modified is closer to the CFD data than the others friction coefficients (Figs. 11-13).

For flame-holders geometries, M1 and M5, there is a drop in Mach number in the cavity region due to the recirculation zone inside it (Figs. 12 and 13).

However, all friction coefficient models fail to accurately predict the temperature distribution (Figs. 14-16). This discrepancy is expected because the region where the chemical reaction occurs is confined near the bottom wall of the combustor. Outside this region, a portion of the flow remains non-reactive, resulting in lower temperatures, dropping the mass-weighted average temperature from CFD (Fig. 17).

Therefore, the Prandtl modified friction coefficient presents the best results when compared with CFD data for the pressure and Mach number. However, it is necessary to improve the low-cost method to account for nonreactive airflow in temperature estimation.

4. Conclusion

This study proposed and evaluated a low-cost methodology for predicting supersonic combustion using a combustion efficiency model calibrated with CFD simulations validated against experimental data. By incorporating viscous effects, the proposed approach estimates flow properties with minimal computational cost. The methodology shows strong agreement with CFD predictions for static pressure and Mach number distributions, particularly when using the Prandtl modified friction coefficient.

However, limitations were observed in temperature prediction due to the confinement of the reactive layer near the wall, which is not fully resolved in the simplified model. Despite this, the low-cost tool demonstrates significant potential for the preliminary design scramjet combustor, enabling rapid assessment of performance trends across a wide design space.

Future work will focus on extending the model's capabilities by developing a generalized correlation for combustion efficiency as a function of equivalence ratio, combustor geometry, and inlet flow conditions. This enhancement aims to improve predictive accuracy while preserving computational efficiency, enabling more reliable preliminary design and optimization of scramjet systems.

Copyright © 2025 by the author(s)

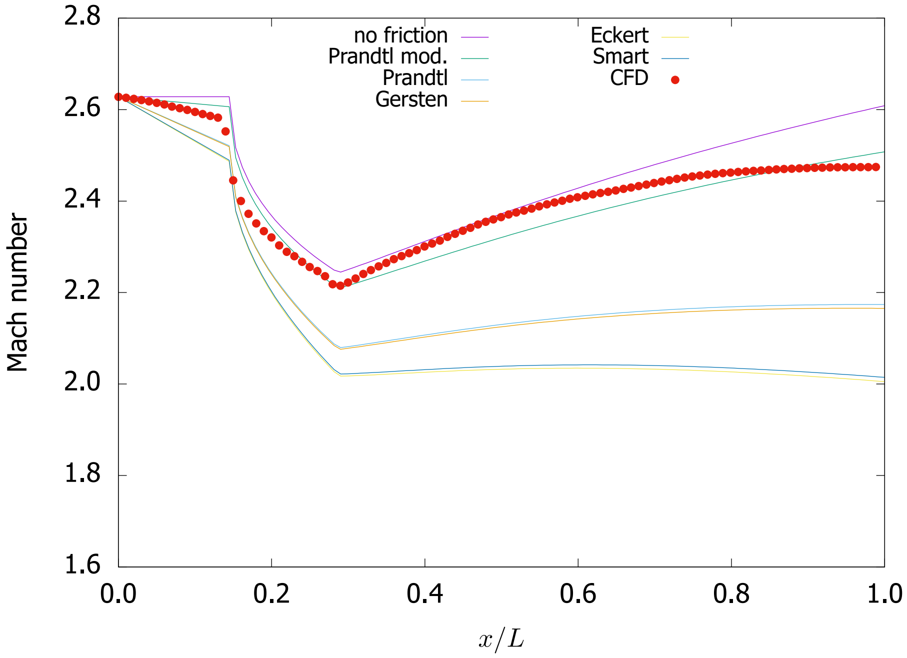

Fig 11. Mach number comparison between CFD and low-cost combustion model for combustor geometry named M0 - CASE I.

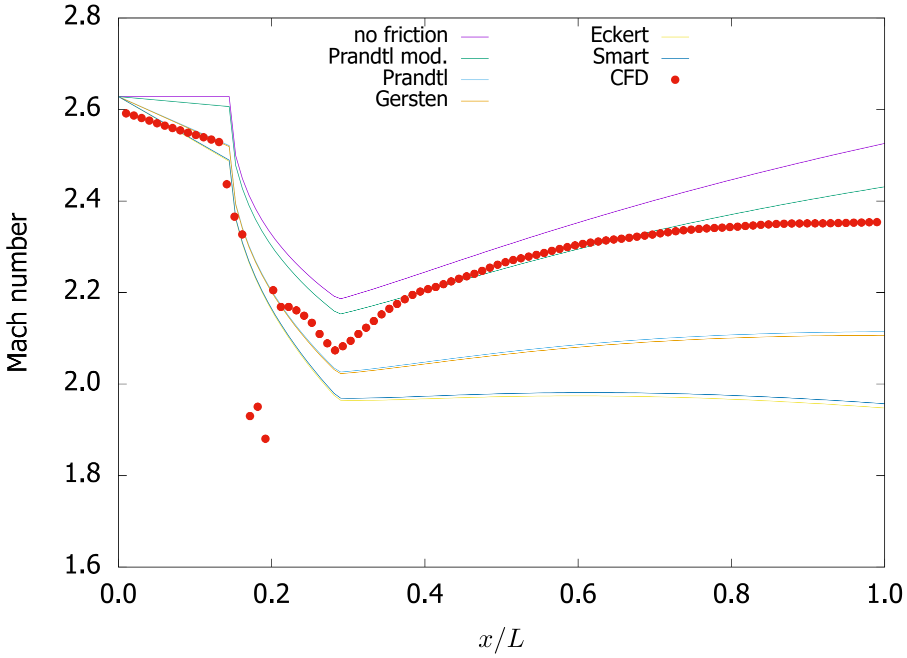

Fig 12. Mach number comparison between CFD and low-cost combustion model for combustor geometry named M1 - CASE II.

Copyright © 2025 by the author(s)

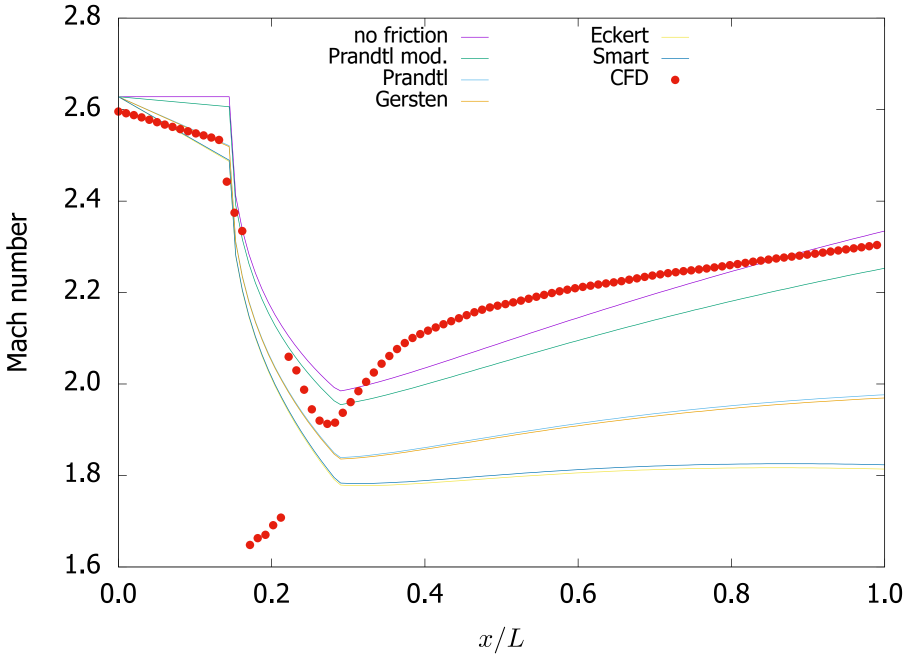

Fig 13. Mach number comparison between CFD and low-cost combustion model for combustor geometry named M5 - CASE III.

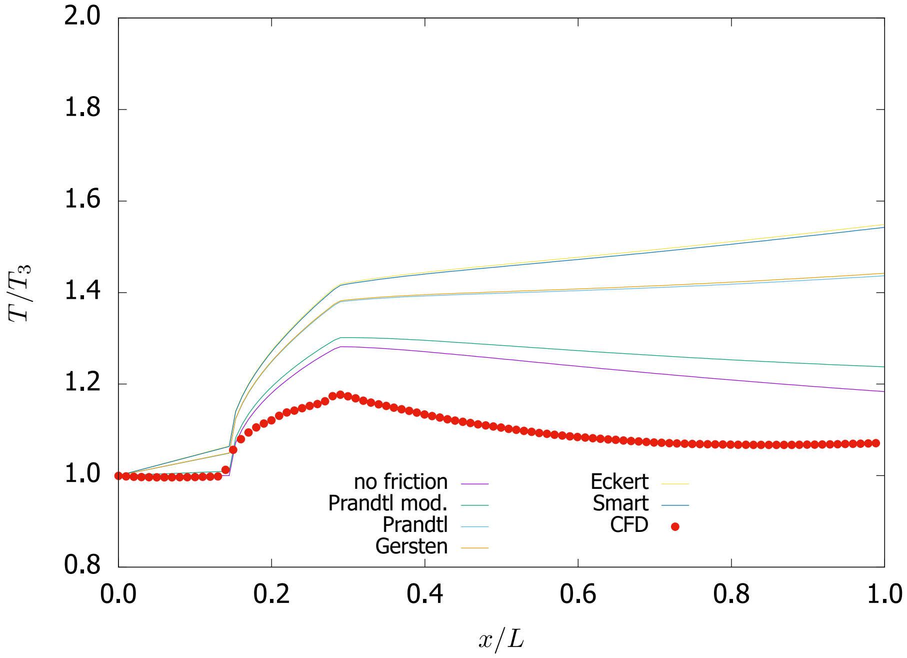

Fig 14. Static temperature comparison between CFD and low-cost combustion model for combustor geometry named M0 - CASE I.

Copyright © 2025 by the author(s)

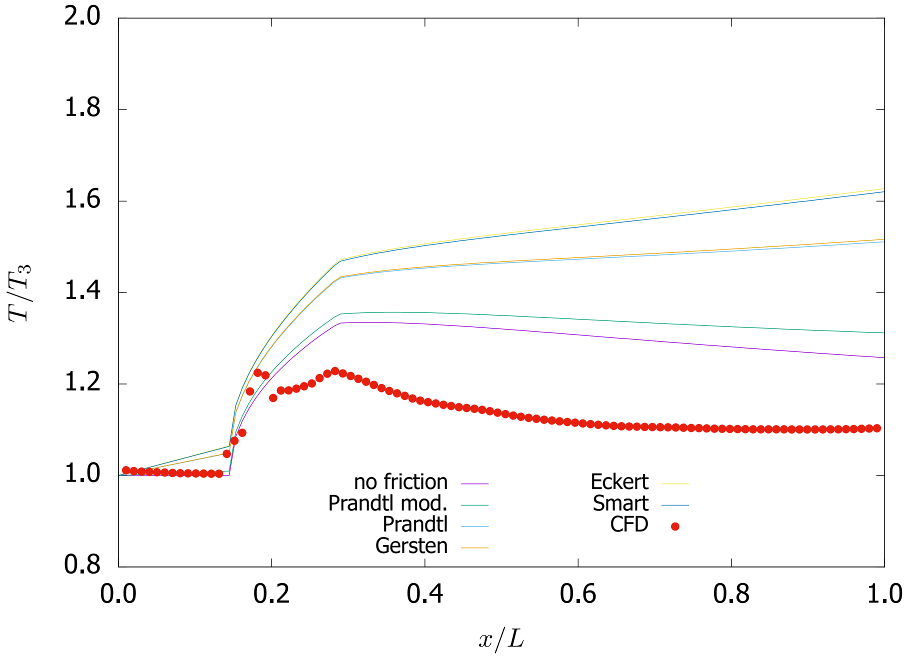

Fig 15. Static temperature comparison between CFD and low-cost combustion model for combustor geometry named M1 - CASE II.

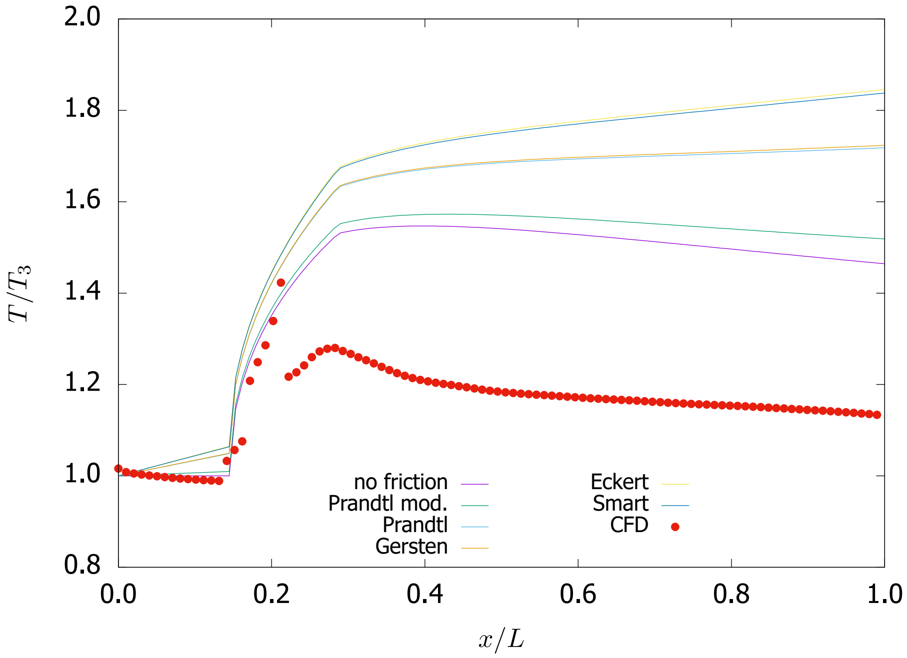

Fig 16. Static temperature comparison between CFD and low-cost combustion model for combustor geometry named M5 - CASE III.

Copyright © 2025 by the author(s)

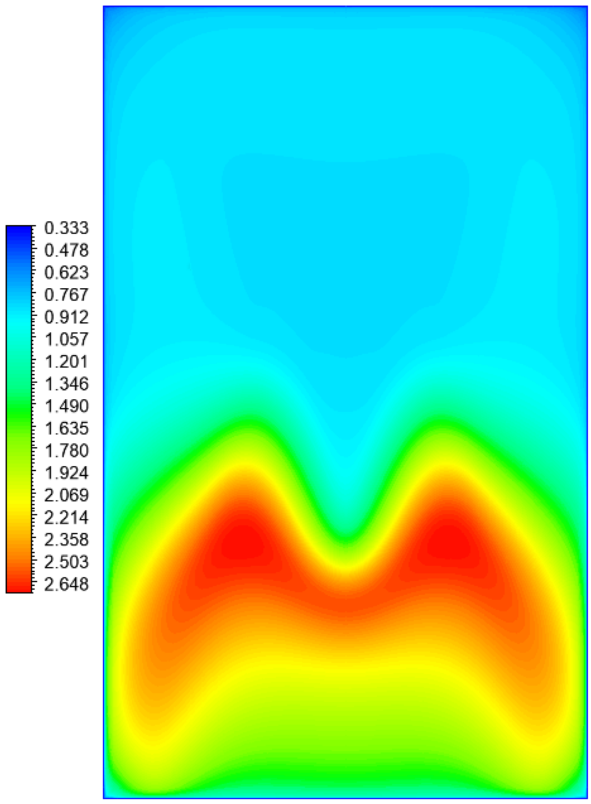

Fig 17. Temperature normalized contour at the outlet for CASE III - M5.

Copyright © 2025 by the author(s)

Acknowledgment
This work was supported by the Brazilian Funding Agency for Studies and Projects (FINEP) under the Contract no.: 01.22.0255.00, by the Brazilian Air Force (COMAER), by the Coordination for the Improvement of Higher Education Personnel (CAPES), under the Contract no.: PROCAD-DEFESA 88881.387753/2019-01, and by Conselho Nacional de Desenvolvimento Científco e Tecnológico under Grant 307691/2020-9;

References
[1] D Anderson Jr. *Modern Compressible Flow - with Historical Perspective*. 2nd ed. McGraw-Hill Publishing Company, 1990.

[2] ANSYS, Inc. *Ansys Fluent Theory Guide*. Release 2021 R2. 15317. ANSYS, Inc. Canonsburg, PA, 2021.

[3] Pedro P. B. Araújo et al. "Multi-objective optimization of a hypersonic airbreathing vehicle". In: *Physics of Fluids* 36.2 (Feb. 2024), p. 026120. ISSN: 1070-6631. DOI: 10.1063/5.0181366. eprint: https://pubs.aip.org/aip/pof/article-pdf/doi/10.1063/5.0181366/19691956/026120_1_5.0181366.pdf. URL: https://doi.org/10.1063/5.0181366.

[4] Pedro P.B. Araújo et al. "Optimization of scramjet inlet based on temperature and Mach number of supersonic combustion". In: *Aerospace Science and Technology* 116 (2021). ISSN: 1270-9638. DOI: https://doi.org/10.1016/j.ast.2021.106864. URL: https://www.sciencedirect.com/science/article/pii/S1270963821003746.

[5] Í. S. A. Bezerra et al. "Influence of the hydrogen transverse injection mode in a scramjet combustor performance". In: *International Journal of Hydrogen Energy* 53 (2024), pp. 1269–1284. ISSN: 0360-3199. DOI: https://doi.org/10.1016/j.ijhydene.2023.11.308. URL: https://www.sciencedirect.com/science/article/pii/S0360319923061475.

[6] Cristian H. Birzer and Con J. Doolan. "Quasi-One-Dimensional Model of Hydrogen-Fueled Scramjet Combustors". In: *Journal of Propulsion and Power* 25.6 (2009), pp. 1220–1225. DOI: 10.2514/1.43716. eprint: https://doi.org/10.2514/1.43716. URL: https://doi.org/10.2514/1.43716.

[7] R. Carneiro, A. Passaro, and P. G. P. Toro. "Heat addition with variable area: Methodology for preliminary design of the scramjet combustion chamber". In: *Physics of Fluids* 35.4 (Apr. 2023), p. 046103. ISSN: 1070-6631. DOI: 10.1063/5.0138781. eprint: https://pubs.aip.org/aip/pof/article-pdf/doi/10.1063/5.0138781/16830242/046103_1_5.0138781.pdf. URL: https://doi.org/10.1063/5.0138781.

[8] R. Carneiro et al. "Leading-to-trailing edge theoretical design of a generic scramjet". In: *AIP Advances* 12.5 (2022). DOI: 10.1063/5.0050786.

[9] E R G Eckert. "Engineering relations for heat transfer and friction in high-velocity laminar and turbulent boundary-layer flow over surfaces with constant pressure and temperature". In: *Transactions of the ASME* 78.6 (1956), pp. 1273–1283. DOI: 10.1115/1.4014011.

[10] P. Gerlinger and D. Bruggemann. "Numerical Investigation of Hydrogen Strut Injections into Supersonic Airflows". In: *Journal of Propulsion and Power* 16.1 (2000), pp. 22–28. DOI: 10.2514/2.5559. eprint: https://doi.org/10.2514/2.5559. URL: https://doi.org/10.2514/2.5559.

[11] William H Heiser et al. *Hypersonic airbreathing propulsion*. AIAA Education Series, 1994. ISBN: 978-1-56347-035-6. DOI: 10.2514/4.470356. URL: https://doi.org/10.2514/4.470356.

[12] William E. Meador and Michael K. Smart. "Reference Enthalpy Method Developed from Solutions of the Boundary-Layer Equations". In: *AIAA Journal* 43.1 (2005), pp. 135–139. DOI: 10.2514/1.2656. eprint: https://doi.org/10.2514/1.2656. URL: https://doi.org/10.2514/1.2656.

[13] F. R. Menter. "Two-equation eddy-viscosity turbulence models for engineering applications". In: *AIAA Journal* 32.8 (1994), pp. 1598–1605. DOI: 10.2514/3.12149.

[14] Hideaki Ogawa and Russell R Boyce. "Physical insight into scramjet inlet behavior via multi-objective design optimization". In: *AIAA journal* 50.8 (2012), pp. 1773–1783. DOI: 10.2514/1.J051644.

[15] L. Prandtl. *Recent Results of Turbulence Research*. Tech. rep. NACA-TM-720. Available at urlhttps://ntrs.nasa.gov/citations/19930094697. Washington, USA: NATIONAL ADVISORY COMUITTEE FOR AERONAUTICS, 1933.

 Copyright © 2025 by the author(s)

[16] H. Schlichting and K. Gersten. *Boundary Layer Theory*. Springer-Verlag, 2004.
[17] Leda Marise Vialta. "Estudo dos efeitos de cavidades abertas em combustores supersônicos". Doutorado em Propulsão Espacial e Hipersônica. São José dos Campos: Instituto Tecnológico de Aeronáutica, 2023, p. 133.
[18] Leda Marise Vialta et al. "Methodology for the application of velocimetry by molecular tagging of hypersonic flows". In: *Flow Measurement and Instrumentation* 88 (2022), p. 102265. DOI: 10.1016/j.flowmeasinst.2022.102265.

Copyright © 2025 by the author(s)